N/P InP Homojunction Solar Cells with an $In_{0.53}Ga_{0.47}As$ Contacting Layer Grown by Liquid Phase Epitaxy*

C. C. Shen and K. Y. Choi

Center for Solid State Electronics Research
Arizona State University
Tempe, Arizona 85287

N/P InP homojunction solar cells with an $In_{0.53}Ga_{0.47}As$ contacting layer were fabricated by liquid phase epitaxy (LPE). Electron-Beam-Induced-Current (EBIC) measurements were performed on several selected samples. It was found that the background doping level in the base region sometimes results in a deep junction, which greatly affects the cell performance.

Introduction

In the past few years we have developed a special contacting scheme in order to facilitate the front grid contact to P/N InP homojunction solar cells [ref. 1, 2]. This contacting scheme utilizes a heavily doped $In_{0.53}Ga_{0.47}As$ layer, which is deposited on the emitter layer during the epitaxial growth cycle. With the aid of the InGaAs contacting layer, very heavy doping at the emitter surface is no more required for obtaining low resistance front contact. The possibility of the formation of "dead layer" at the front surface is therefore eliminated. In this work, we extended this contacting scheme to N/P InP homojunction solar cells grown by LPE. The LPE growth procedures, cell fabrication and experimental results are presented in the following sections.

Cell Fabrication

The schematic diagram of the N/P homojunction InP solar cells developed in this work is shown in Fig. 1. The LPE growth was performed in a conventional horizontal LPE system, which employs a multiple-bin sliding graphite boat for multiple-layer growth.

The starting material was a (100) oriented p^+-InP single crystal substrate which had been polished previously into a mirror-like surface by chemical-mechanical method. Three epitaxial layers were grown successively onto the substrate. A p-InP base layer of several microns thick was first grown on the substrate, which was followed by a thin n-InP emitter layer and a thin n^+-InGaAs contacting layer. Zinc was used as p-type dopant and tellurium was used as n-type dopant. The typical growth temperature was between 622°C and 638°C, with a cooling rate of 0.5°C/min.

Selected grown wafers were processed into mesa-type solar cells. The processing sequence used in this work is similar to what we used for P/N InP homojunction solar cell [ref. 1]. The total area of the cells processed in this work are of two different sizes; they are 0.04 cm² and 0.25 cm². The

i

front grid contact covers 6% and 12.5% of the total surface area for 0.25 cm^2 size cells and 0.04 cm^2 size cells, respectively. ZnS/MgF$_2$ double-layer AR coating was deposited on the front surface by thermal evaporation.

Electron-Beam-Induced-Current (EBIC) Measurements

EBIC measurements were performed routinely on broad-area diodes processed from grown wafers. It is a useful technique for determining the exact location of the p-n junction in a junction device such as a solar cell. During the course of this study, we had some interesting observations from the EBIC data on several grown wafers which were prepared under slightly different growth conditions. Our findings are described below.

Several LPE samples were grown under similar growth conditions. Doping level in the p-InP base region was adjusted by varying the Zn content in the melt used for growing the base layer. For this particular series of growth experiments, the melt was not intentionally baked for any prolonged period of time prior to the growth to minimize the background doping.

In Table I, we list the LPE growth recipes we used for the preparation of two samples (sample A and sample B), both contain a N/P InP homojunction and a n$^+$-InGaAs layer. The targeted doping levels in the base region for these two samples are 5×10^{16} cm^{-3} for sample A and 1×10^{17} cm^{-3} for sample B.

Both samples were made into broad-area devices. Devices with rectifying I-V characteristics and smooth cleaved-facets were selected for EBIC studies. To delineate the InGaAs/InP interface, the diodes to be tested were first etched in a solution of 3H$_2$SO$_4$: 1H$_2$O$_2$: 1H$_2$O at room temperature for 20 sec. The SEM photomicrographs of the cleaved and etched section of two diodes are shown in Fig. 2(a) and 2(b). The photomicrograph shown in Fig. 2(a) was taken from a diode processed from sample A while the one in Fig. 2(b) was from a diode processed from sample B. The heterojunction interface between the InGaAs contacting layer and the InP emitter layer is revealed in the secondary emission image. The location of the p-n junction is identified by the peak of the superimposed beam-induced current trace. For sample B, the p-n junction is about one micron from the InGaAs/InP interface as expected. However, the p-n junction in sample A, as revealed in the EBIC photomicrograph, is four microns from the InGaAs/InP interface. Our explanation for this striking result is that in sample A, the n-type background doping in the base region was higher than the targeted p-doping; as a result, the amount of Zn incorporated in the melt for the growth of the p-base layer was not enough to overcome the background doping and the base layer turned out to be n-type instead of p-type, resulting in a p-n junction between the first epitaxial layer and the p$^+$-InP substrate. Such a deep junction is not desirable because it will result in low short-circuit current. The background doping in the base region for sample A was estimated to be in the high 10^{16} cm^{-3} range, as measured by a Polaron profile plotter. Since no pre-bakeout of the melts were employed in this particular growth experiment, high level of background doping was obtained. In order to avoid this problem, proper pre-bakeout of the melts prior to growth is definitely necessary.

Cell Performance

The spectral response of two representative cells, one processed from sample A (cell A) and the other from sample B (cell B), are shown in Fig. 3(a) and 3(b). The external quantum efficiency of cell A in the short wavelength region is relatively low in comparison to that of cell B. This result is not surprising, since cell A has a deeper junction and optically generated carriers near the cell surface are not collected efficiently. It is worthwhile to point out that for the two cells discussed here, their cell structures are far from optimized. The peak value of the quantum efficiency for both cells are therefore quite low.

Figure 4 shows the dark I-V characteristics for these two cells. Cell A exhibits very poor dark I-V characteristics, which might be caused by the poor quality of the junction formed between the epitaxial layer and the substrate. The cells were tested under simulated AM1 illumination and their light I-V characteristics are shown in Fig. 5. The conversion efficiencies for cell A and cell B are 2.0% and 9.8%, respectively. The photovoltaic properties of cell A and cell B under AM1 illumination are summarized in Table II. These two cells have a total surface area of 0.25 cm^2. Total-area conversion efficiencies up to 13.5% at AM1 was obtained from a small cell with a total surface area of 0.04 cm^2. The smaller cell also exhibits higher V_{oc} and larger fill factor.

A comparison between N/P and P/N homojunction InP cells grown by LPE growth techniques at our laboratory indicates that the short-circuit current for N/P InP cells seem to be more sensitive to the emitter thickness. In order to achieve high conversion efficiency for N/P InP cell, the emitter layer needs to be very thin, probably in the order of 500Å.

Conclusion

We have prepared N/P InP homojunction solar cells with an n^+-$In_{0.53}Ga_{0.47}As$ contacting layer by LPE growth techniques. EBIC studies showed that the high background doping in the base region can create a deep p/n junction, which greatly affects the cell performance. Pre-bakeout of the growth melts is required if low doping concentration in the p-base region is desired for the preparation of N/P InP homojunction solar cells by LPE growth techniques. N/P InP homojunction solar cells grown by MOCVD growth techniques may encounter similar problems if the background doping level in the epitaxial InP layer is high due to impure sources or system contamination. EBIC measurements can therefore serve as a useful diagnostic tool for investigating this particular problem.

For the N/P InP homojunction solar cells described here, both the LPE growth procedures and the cell parameters need to be improved and optimized in order to obtain higher conversion efficiencies. Adding a buffer layer may improve the quality of the epitaxial layers and the p/n junction quality.

References

[1] K. Y. Choi, C. C. Shen and B. I. Miller, "P/N InP Homojunction Solar Cells by LPE and MOCVD Techniques", *19th IEEE Photovoltaic Specialists Conference*, New Orleans, LA, 1987, Conf. Rec., pp. 255-260.

[2] K. Y. Choi and C. C. Shen, "P/N InP Homojunction Solar Cells with a Modified Contacting Scheme by Liquid Phase Epitaxy", J. Appl. Phys. **63**, no. 6, Feb. 1988, pp. 1198-1202.

Table 1. LPE growth recipes for sample A & B.

Growth recipe for sample A

Layer	In (gm)	InP (mg)	GaAs (mg)	InAs (mg)	Zn (ug)	Te (mg)	Growth Temp.	Growth Period	Expected Carrier Concentration (cm^{-3})
p-InP	1.0	9.0	----	----	1.5	---	$638.0^{o}C$	30 min	5×10^{16}
n-InP	1.0	7.0	----	----	---	2.2	$623.0^{o}C$	10 sec	5×10^{18}
n^{+}-$In_{0.53}Ga_{0.47}As$	1.0	---	30.9	50.9	---	4.0	$622.8^{o}C$	3 sec	1×10^{19}

Growth recipe for sample B

Layer	In (gm)	InP (mg)	GaAs (mg)	InAs (mg)	Zn (ug)	Te (mg)	Growth Temp.	Growth Period	Expected Carrier Concentration (cm^{-3})
p-InP	1.0	9.0	----	----	1.7	---	$638.0^{o}C$	30 min	1×10^{17}
n-InP	1.0	7.0	----	----	---	2.0	$623.0^{o}C$	10 sec	4×10^{18}
n^{+}-$In_{0.53}Ga_{0.47}As$	1.0	---	30.9	51.6	---	4.0	$622.8^{o}C$	3 sec	1×10^{19}

Table 2. Photovoltaic and electrical characteristics of N/P homojunction InP solar cells under AM1 illumination.

ELH lamp, 100 mW/cm^2, 27°C

Cell area: 0.25 cm^2

Sample	V_{oc} (V)	J_{sc} (mA/cm^2)	FF (%)	Eff. (%)	n factor	J_o (A/cm^2)
A	0.72	6.0	46.8	2.0	10.2	1.5×10^{-4}
B	0.82	20.8	57.6	9.8	2.8	1.8×10^{-7}

MgF$_2$/ZnS AR Coating

Front Grid Contact

n^+-In$_{0.53}$Ga$_{0.47}$As

n-InP

p-InP

p^+-InP Substrate

Back Contact
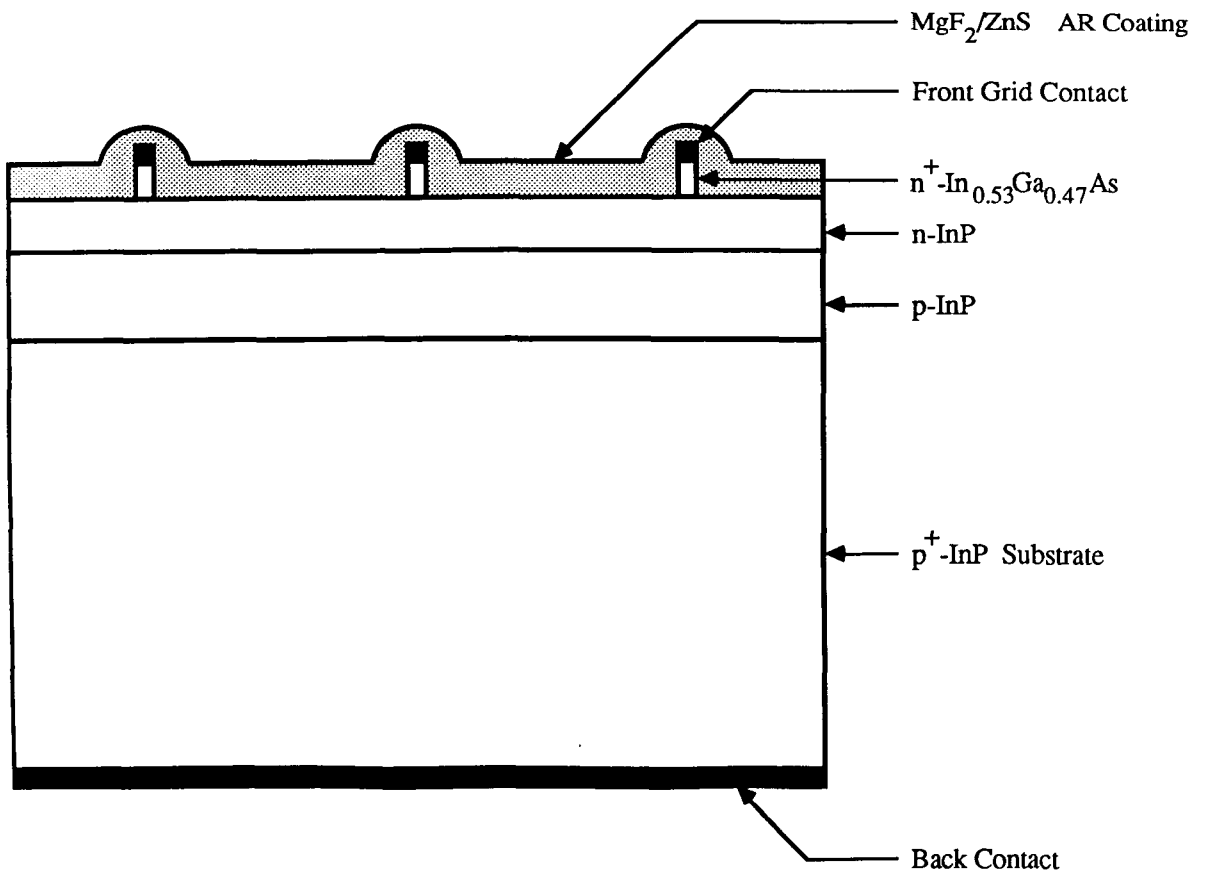
Figure 1. Schematic diagram of the cross section of an N/P InP homojunction solar cell.
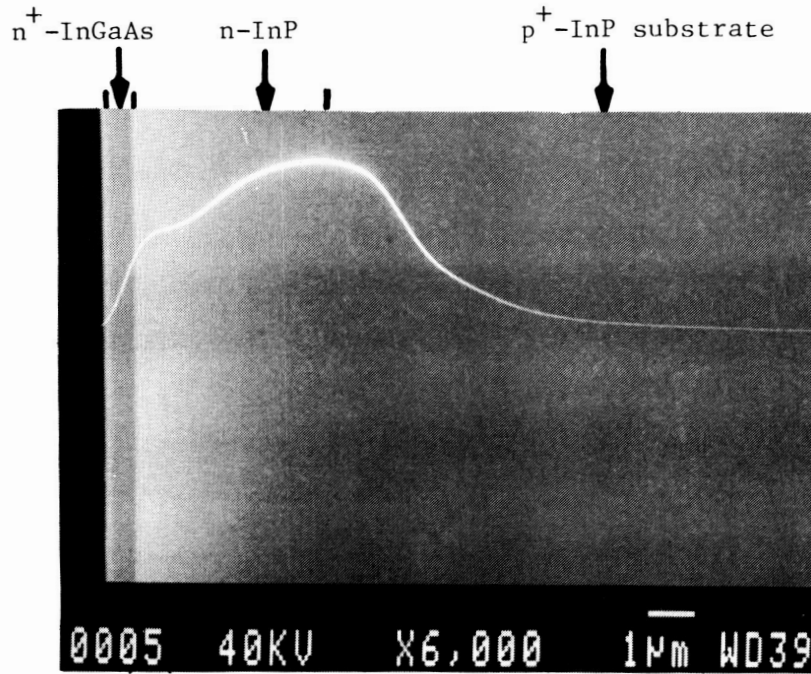
(A)
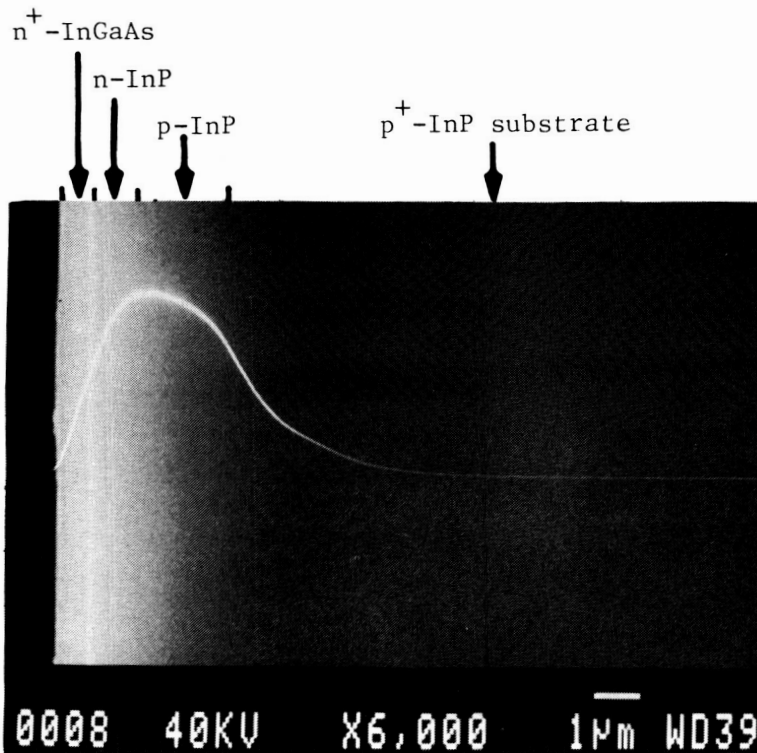
(B)

Figure 2. Secondary emission and EBIC images of the cross section of
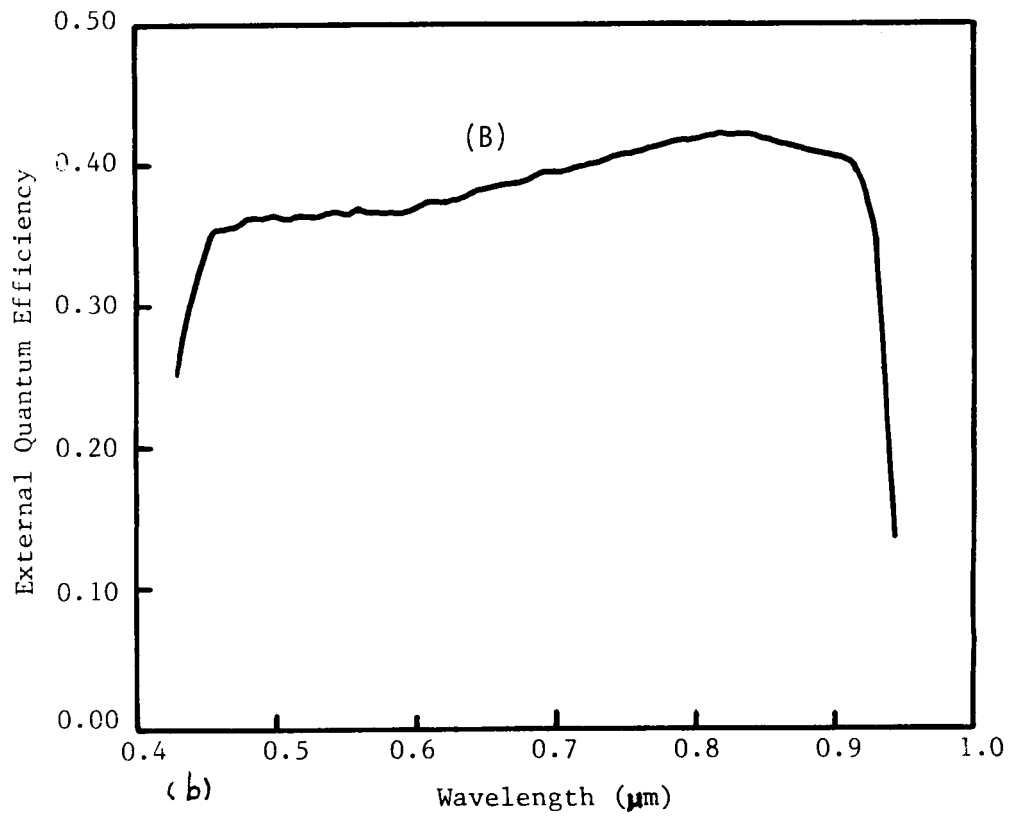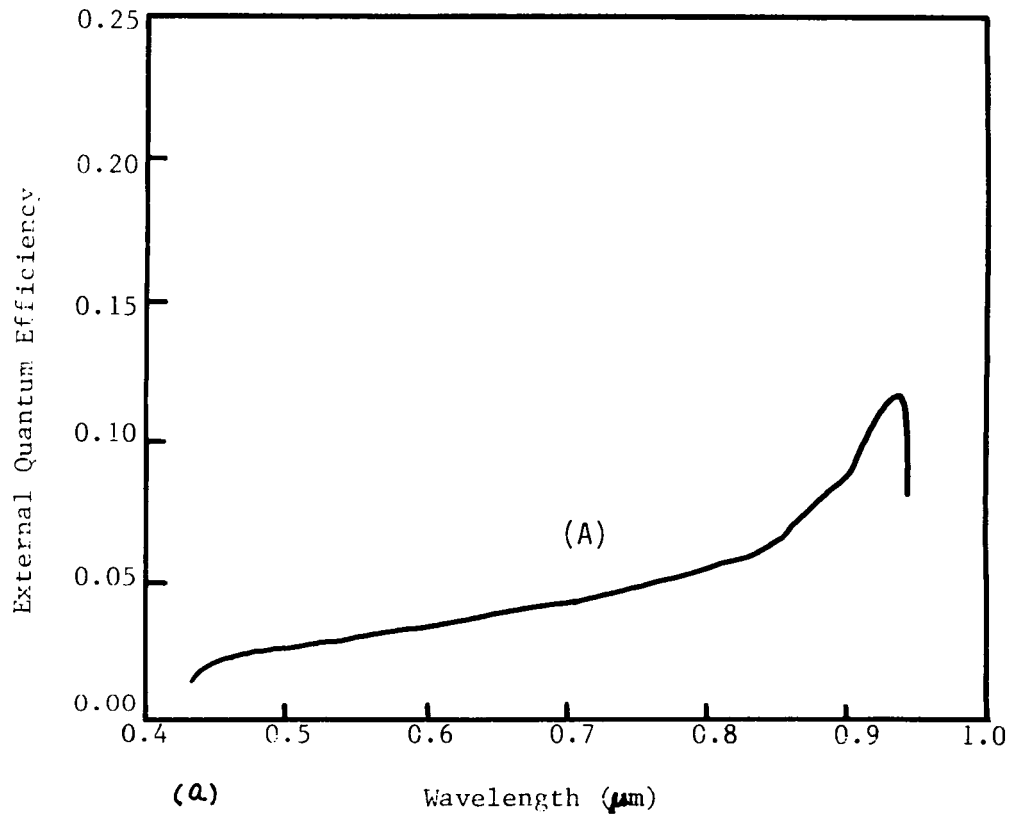(A) Cell A and (B) Cell B.

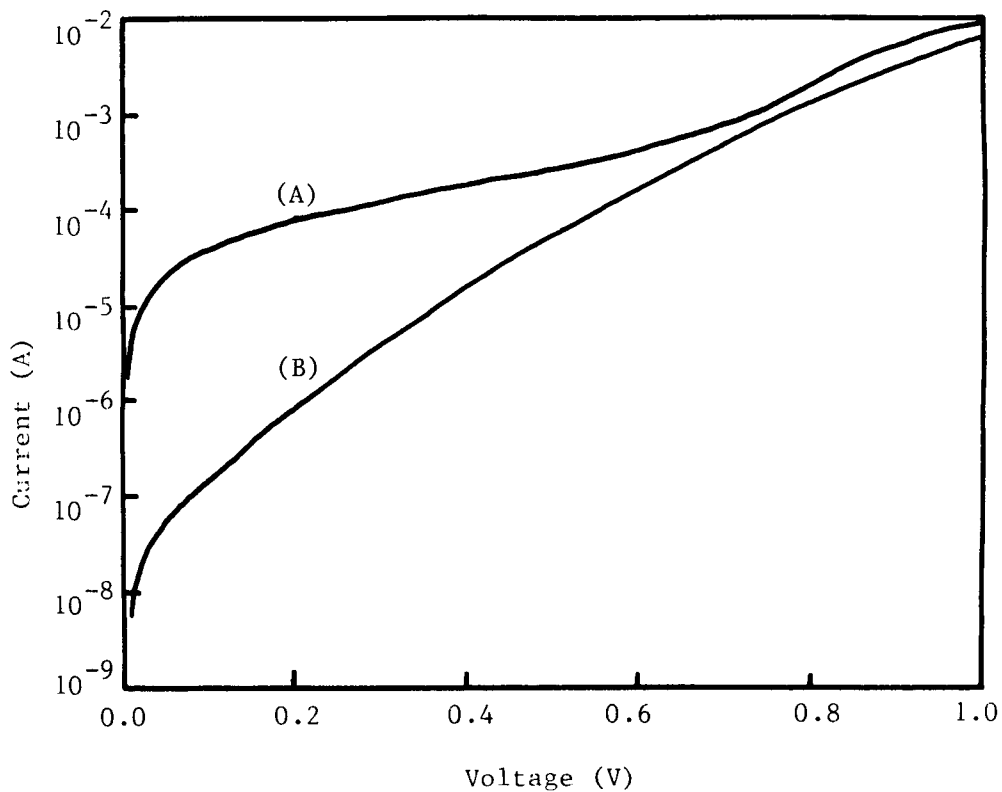Figure 3. Spectral response of (A) Cell A and (B) Cell B.

Figure 4. Dark I-V characteristics of (A) Cell A and (B) Cell B.
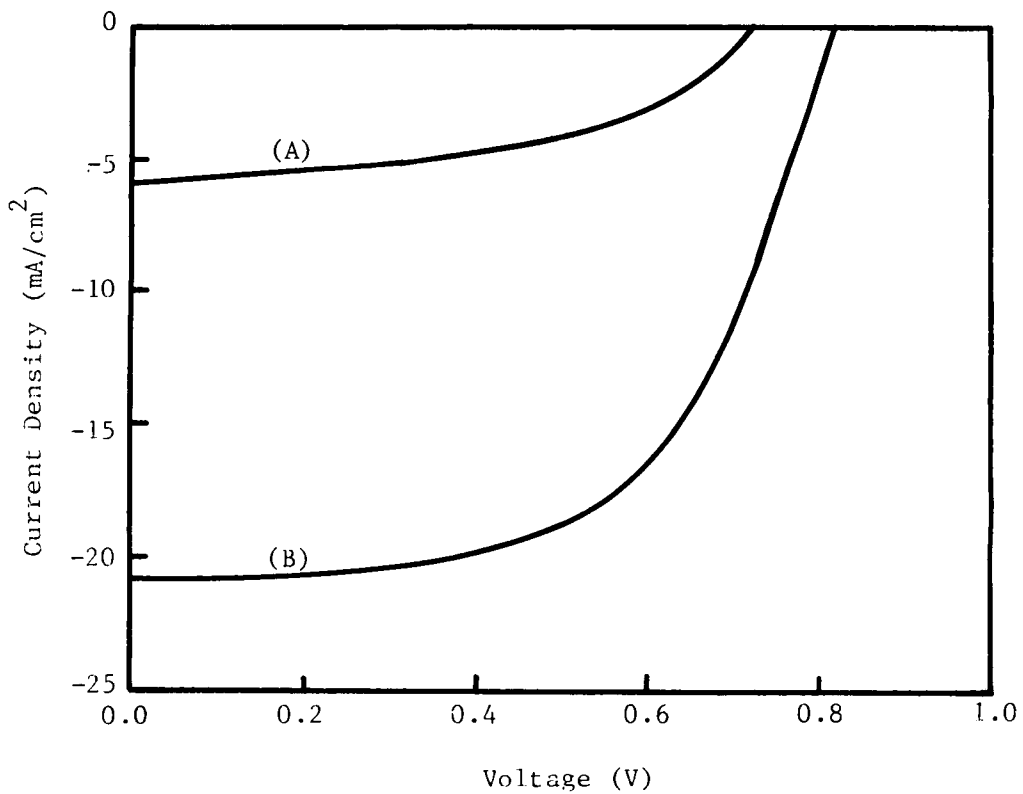

Figure 5. Light I-V characteristics of (A) Cell A and (B) Cell B under AM1 illumination.